Int. J. Nanosci. Nanotechnol., Vol. 19, No. 3, Sept. 2023, pp. 199-207
DOI: 10.22034/ijnn.2023.562891.2285

Short Communication

An Experimental Investigation of Deposition of ZnS Materials on Glass Substrate with SILAR

Haytham El Farri*, Amal Yousfi, Mounir Fahoume, Lahoucine El Gana and Latifa Znaidi

Department of Physics, Faculty of Sciences, University Ibn Tofail, BP 14000, Kenitra, Morocco

(*) Corresponding author: haythamelfarri@gmail.com
(Received: 02 October 2022 and Accepted: 04 August 2023)

Abstract

The formation of zinc sulfide (ZnS) is the most promising semiconductor material, particularly for optical and photovoltaic applications. The influence of the number of cycles on ZnS thin films deposited at room temperature was studied. According to our findings, the results showed that the number of deposition cycles affected the crystallinity, grain size, film thickness, and shape of the obtained films. The XRD analysis confirmed that the thin films fabricated had a crystalline structure of zinc blend ZnS with a preferred orientation in the plan (111). The gap energy of ZnS has been obtained in the range of 3.34 eV to 3.68 eV.

Keywords: *SILAR, ZnS, XRD, Band gap energy, Sulfurization, SEM.*

1. INRODUCTION

In last decades, binary semiconductors have been studied in an effort to discover novel materials to improve the efficiency of solar energy conversion [1]. This renewable energy is considered as the most abundant on our planet. Many researchers have found that the chalcogenide materials present interesting semiconductor properties as buffer layer and window layers in photovoltaic applications. The study on this group of elements in the periodic table has increased due to their diverse applications, according to the researches elaborated by Shobana et.al [2]. Naghavi et al have reported that binary compounds of chemical elements play a major role in optoelectronic devices, especially in solar cells second generation constituted by these materials for window layer and buffer layer [3]. F. Rahman et al. have studied many applications of binary chalcogenide semiconductors to solar cells such as non-linear optical devices and light-emitting diodes (LEDs), which was confirmed by A.Yildiz et al [4, 5]. The figure below shows a cross section of CIGS based solar cells, deposited on glass substrate [6].

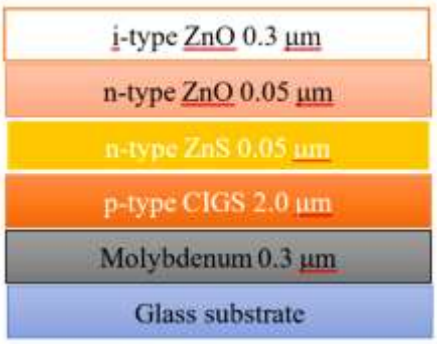

Figure 1. *Cross model image of CIGS solar cells deposited on glass substrate of nanoparticles.*

On this cross section, the absorber material is deposited atop the Molybdenum (Mo) back contact electrode [7]. Then, the heterojunction is completed by a Zinc Sulfide (ZnS) material (Buffer layer), n doped and an undoped Zinc Oxide (intrinsic) i-ZnO (window layer) respectively [8]. The back contact layer (Mo) and front contact layer relieve the charge transport from the p-n junction. ZnS presents a combination of II-VI group semiconductors and finds many applications in lasers, photovoltaic devices, luminescent displays and solar cells [9]. In other models of photovoltaic cells, CdS was used as buffer layer, but in reason of its toxicity to the environment, the experimental researches have been elaborated to study the possibility of replacing CdS with alternative materials, which is our case. Besides, CdS has small large of gap energy which is the principal reason of lost many light photons of energy up of its gap 2.42 eV [10]. As first propositions, some researchers have studied and proven that the binary materials of the same group of crystal (II-VI) in the periodic table can be candidates of CdS thin films. For our part, we studied the replacing of CdS material by ZnS material, with effect of experimental parameter called number of cycles, which will be developed in experimental part of this work. This binary semiconductor is characterized by its larger band gap than CdS. Some studies have investigated a theoretical simulation of ZnS for photovoltaic applications, proved in the paper of H. Elfarri et al, which explain the theoretical reason of using ZnS in solar cells devices [11]. In conclusion of these studies, they noticed that ZnS Buffer layer can constitute an alternative material to CdS, and its application is more useful than CdS in the region Blue light [8]. I.H.Nisreen et al have based them study on the concept that ZnS has two crystalline structures: zinc blende (cubic phase) and wurtzite (hexagonal phase) with bandgap energies of 3.54 and 3.80 eV, respectively [12]. The band gap energy characteristics of ZnS make it useful in thin-film electroluminescent devices. A lot of studies have confirmed a versatile solution approach for different metal Sulfide thanks to the easy availability and low cost of the primary materials. Additionally, ZnS offers great multifunctionalities in various optoelectronic applications. Multiple physical and chemical techniques have been used to synthesis ZnS thin film Among these techniques, due to its simplicity and its low cost: SILAR technique offers the opportunity to control the material properties of ZnS compound, by varying parameters such as the concentration of precursors, immersion time, rinsing time, pH values, and number of SILAR cycles [13]. We will study the influence of number of cycles on the structural, morphological and optical properties of this suggested material. The properties of this material deposited on a glass substrate have been historically introduced for the first time by Nicolau in 1985 through the SILAR method for the deposition of thin films [14]. Its criteria are based on the successive reaction of solvated ionic compound on the solution solid interface. SILAR technique was chosen for our work thanks to its simplicity and its economical coast [15]. Besides, it doesn't need much expansive primary materials for deposition of binary compounds, and all experimental process of this technique passed at room temperature, which explains its security for the environment study.

2. EXPERIMENTAL PHASE

The Zinc Acetate Zn $(CH_3COO)_2$ was dissolved in deionized water to make a 0.1M solution of cationic precursor, while the sulfide Sodium Na_2S was dissolved in distilled water to make a 0.1M of anionic precursor S^{2-}. The Ammonium hydroxide

NH_4OH was used as a complexing agent to prevent precipitation of Zn^{2+} and S^{2-}. For each number of cycles, we obtained ZnS sample as thin films deposited on glass substrate. These samples were characterized by an XPERT-3 X-ray diffractometer with monochromatic Cu-Kα1 radiation λ = 1.5406 Å. The surface morphology and composition of the deposited thin films were determined using scanning electron microscopy (SEM) equipped with an energy–dispersive X-ray spectroscopy (EDS). For optical properties, the JASCO V-670 spectrophotometer was used to measure the absorbance spectra with a wavelength range 335 to 1100 nm. We improved the number of SILAR cycles (30,40 and 50 cycles) to define their effect on the optical and structural properties of the deposited ZnS. Then, we characterize them using X- ray diffraction, scanning electron microscopy (SEM-EDS) and UV-VIS spectrophotometer. These character-izations were used to determine the structural, morphological, and optical properties of the films with the aim of ascertaining the effect of number of cycles on the optoelectronic properties of our material (ZnS). Some works have studied the effect of this parameter with much number (150 to 300 cycles) then us. Ashith et al have studied the maximal of number of cycles with no identification to phases group of ZnS in 50 cycles, contrary to the results obtained in our work [16]. The performance of our samples has been elaborated thanks to a tubular furnace used to ameliorate the crystalline structure of ZnS samples. This tubular has supported many samples obtained in high quality with minimal number of cycles, what was reported by M.Bouachri et al [13].

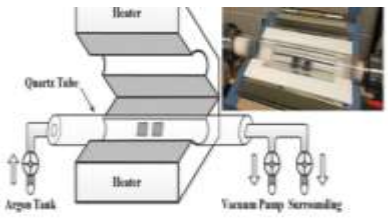

Figure 2. *Tubular furnace used for the annealing process.*

3. RESULTS AND DISCUSSIONS

3.1. Structural Studies: XRD Patterns

The structural parameters of ZnS thin films are given in Table 1. We use the Scherrer formula to calculate the crystallite size of the films. Figure 3 shows typical XRD patterns for films containing on different immersion cycles (30, 40 and 50 cycles). The diffraction peaks can be indexed to a cubic phase (Blend) with preferential orientation to the plane (111), which has the highest intensity and is in good agreement with the standard Data card (JCPDS #80-0020) and with other reports [17]. As we can notice from the XRD patterns, the intensity increases relatively with the increasing number of immersion cycles, which shows an improvement in crystallization. The XRD parameters are given in Table 1.

Table 1. *The structural parameters of ZnS thin films with different dipping cycles number.*

Number of Cycles	Miller Indices (hkl)	Bragg's Angle (2θ)	d spacing (Å)	β (10^{-3} rad)	Crystallite size (nm)
30 Cycles	(111)	28.3367	3.1574	09.61	15.535
	(220)	47.3288	1.9124	08.24	19.181
	(311)	56.2369	1.6334	10.04	16.345
40 Cycles	(111)	27.9890	3.1921	05.49	27.175
	(220)	46.9702	1.9244	06.87	22.974
	(311)	55.8842	1.6418	10.05	16.303
50 Cycles	(111)	28.5946	3.0997	04.81	31.055
	(220)	47.5285	1.9018	04.12	38.387
	(311)	56.4242	1.6240	06.70	24.516

As shown in the figure below, the diffraction peaks of ZnS thin films become more pronounced for the synthesized samples. The patterns samples show polycrystalline structure with a cubic phase structure of β-ZnS and peaks are corresponding to (111), (220) and (311) planes. However, all synthesized ZnS nanoparticles shown a preferential

orientation of the crystallites along the (111) direction [18]. We can notice that that the crystallite size is dependent on the number of cycles of SILAR Technique

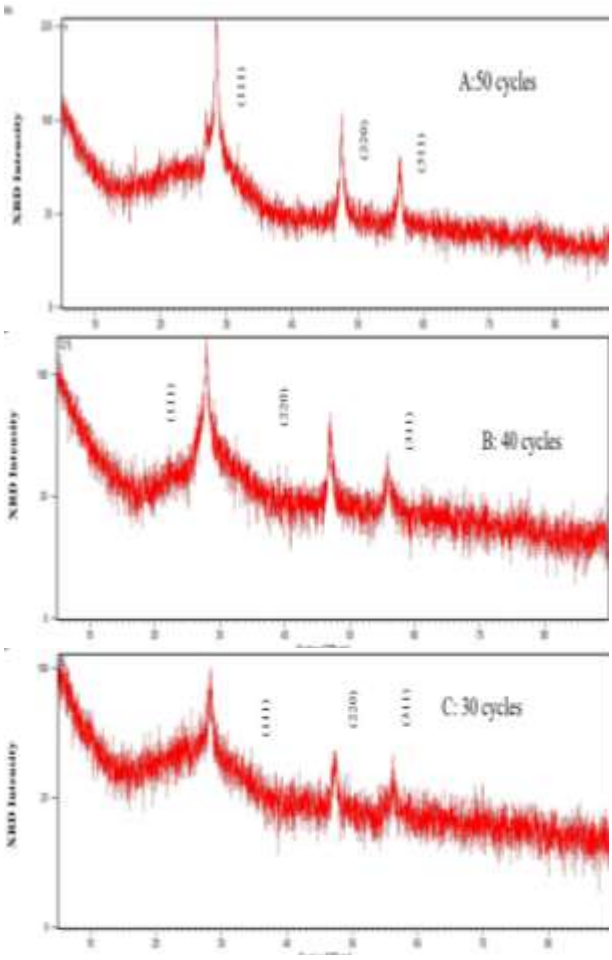

Figure 3. *The XRD spectra of deposited ZnS in diferent number of cycles: A 30 cycles, B 40 cycles and C 50 cycles.*

However, when that parameter decreases, the Zn^{+2}: S^{2-} molar ratio increases, as the Sulphur concentration increases the crystallinity and the crystallite size of the ZnS. At 50 cycles, we notice that the concentrations of Sulphur increased, which was due to the availability of Zn^{+2} and S^{2-} ions, more nanoparticles were formed, resulting in larger particle size. By changing the molar ratio of Zn^{+2}: S^{2-}, we can control the particle size of ZnS nanoparticles as shown in the figure 4.

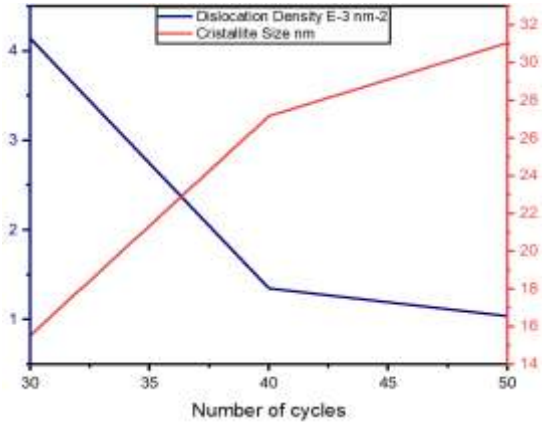

Figure 4*. Dislocation density and crystallite size change with different number of cycles.*

3.2. Morphological Properties: Scanning Electron Microscope and EDX Analyses

The surface morphology of ZnS thin films in three samples was a whitish, uniformly distributed coating on the surface of the glass substrate. The SEM images are shown in Figure 5, where we visualize the surface structure of ZnS. We also noticed that there are voids in every sample for each number of cycles, and they are decreasing with increasing of SILAR cycles. That indicates a denser structure appearing in ZnS thin films with variation of the molar Zn:S ratio. In addition, sample (a) mentions a relative discontinuity emerged on the sample surface, which probably leads to a possible leakage current, if it is used as a buffer layer in second-generation solar cells. Contrary to samples (b) and (c), the coalescence of grains was improved and the Zn:S ratio increased with the number of deposition cycles, thanks to an increase in surface adhesion, which is considered the most important factor for photovoltaic applications. We can see that when the number of cycles increases, the grains are diffused uniformly in an irregular shape and size, which is in agreement with other results obtained by K.S.Ojha [19]. Figures 5 (a), (b), and (c) show the SEM micrographs of ZnS samples for 30, 40 and 50 cycles respectively. The EDX spectra of ZnS thin films produced at 30, 40, and 50 cycles show the presence of two important

elements, Zn and S, constituting the ZnS film with different and high intensities. We also noted the presence of other elements in the spectrum, such as Carbone C, which originated probably from the precursor of $ZnCH_3CO_2H$, which was not completely consumed. We also note the presence of Oxygen O, in considerable quantity, which could be originating from the glass substrate.

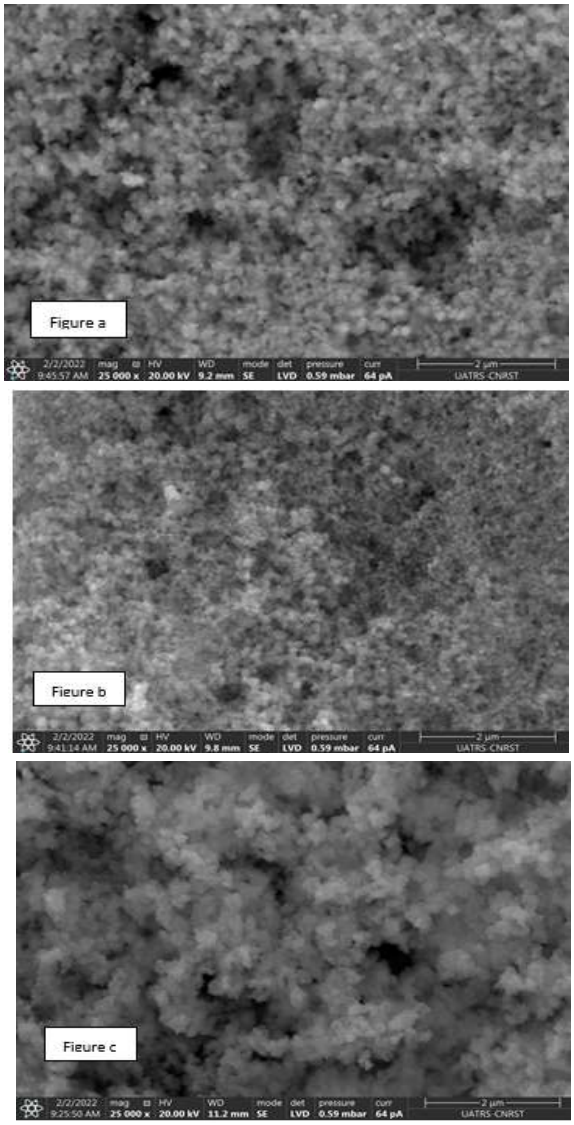

Figure 5. *SEM micrographs of ZnS at (a) 30 Cycles (b) 40 Cycles and 50 Cycles (c).*

From these spectra, we noted that the atomic percentage of sulfur increases with the increase in the number of cycles, indicating that the surfaces of the thin films of ZnS are rich in sulfur. However, when the number of cycles increases, the thickness of the film and sulfur level increase. We have informed the variation of the Zn/S ratio as a function of the number of cycles; the Zn/S ratio is lowered with a decrease in the number of ZnS deposition cycles, which is probably due to the migration of sulfur from the volume form to the surface form of the film, which conforms to the investigations of the DRX elaborated by M.Asghar et al. [19]. To confirm chemical composition of ZnS nanoparticles, we used EDX analysis. We have reported a typical EDX spectra of ZnS-films deposited by SILAR technique as a function of cycle number. The EDX graphs of ZnS produced at 30, 40 and 50 cycles show the presence of two important elements, Zn and S, constituting the ZnS film [20].

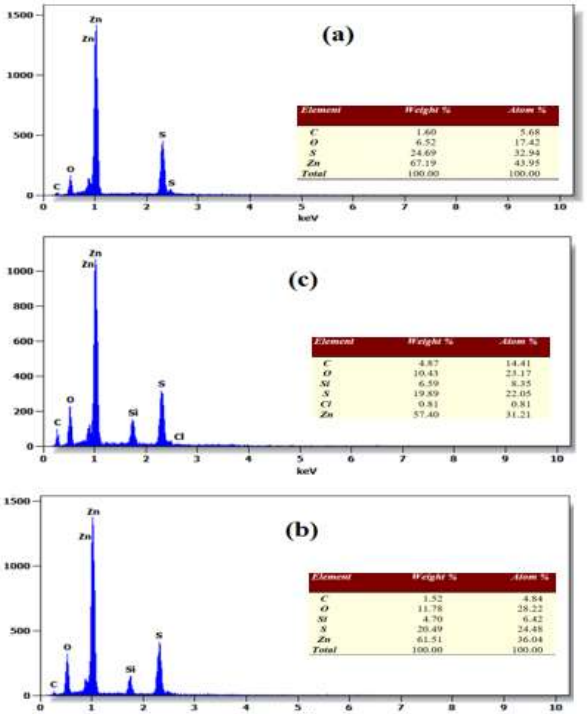

Figure 6*. Analysis spectra of EDX with the chemical composition of each case of number of cycles: 30 (7a), 40 (7b) and 50 (7c) cycles.*

3.3. Optical Properties: UV-VIS Spectroscopy

UV-VIS spectroscopy refers to the transmission and absorption spectroscopy

in the ultraviolet-visible spectral region. Using annealing at high temperature with sulfurization makes ZnS nanomaterials thicker and more composite with low light transmission values**.** When we plot $(\alpha hv)^2$ versus (hv) and extrapolate the linear region of the resulting curve, E_g can be obtained. The band gap energy is determined from this graph. The linear nature of the plot of absorbance indicates that a direct transition is occurring in the ZnS semiconductor. [21]. The study of optical absorption leads to the explanation of the band gap energy of ZnS [22]. The figure 7 demonstrates the variation of optical absorbance at different numbers of cycles. From the plots, we can notice that absorbance decreases in the near infrared region, indicating high absorbance for all samples of ZnS and low transmittance in the visible region, which is confirmed in the work reported by F.G.Beker et al [23]. The ZnS nanofilms can absorb light quanta with energy hν, reduced than E_g. Light absorption at $h\nu < E_g$ may be associated with wide size distribution of ZnS nanoparticles or with high defects concentration in the lattice of ZnS nanocrystals. The band gap of each sample was found 3.68eV, 3.49eV and 3.34eV for 30 cycles, 40 cycles and 50 cycles respectively. Generally, the optical band gap is affected by charged impurities, residual strain and particle size confinement. [24]. A compressed lattice of the film produces a compressive strain which creates an increase in the optical band gap. On the other hand, the elongated lattice leads to a tensile strain which decreases the band gap. From the results obtained on DRX, the film crystallinity increases with an increasing number of cycles, whereas the thickness is obtained, the particle size at this moment increases, which probably reduces the band gap energy of our films. After the sulfurization process at 400 C into the tubular furnace, the crystal lattice expands and the interatomic bonds become weakened. This weakness is responsible to break a bond and create a couple electron-hall.

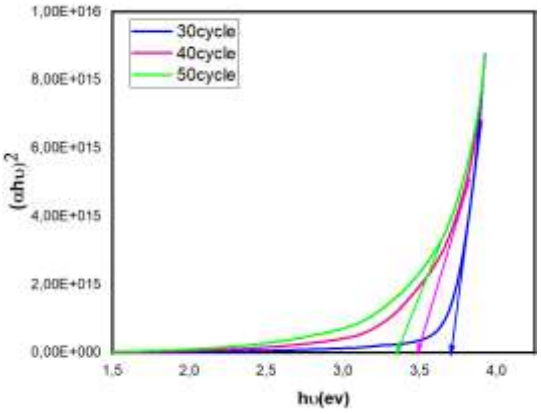

Figure 7*. Plot of Absorbance of ZnS thin films with SILAR technique, for 30, 40 and 50 cycles.*

3.4. FTIR Spectroscopy

FTIR spectra is a simple technique used in order to identify some functional groups pertaining to ZnS. The technique was done to confirm ZnS formation. Its principle is based on exposure of a material to be analyzed to an infrared beam in the number domain waves generally between 400 and 4000 cm^{-1} and the recording of the fraction of the energy of this electromagnetic radiation absorbed by the material. This fraction of the wave is absorbed when its energy coincides with the vibration energy of the inter-band. When we studied the FTIR spectra of ZnS samples, we noticed that the FTIR spectra are same and are presenting in figure 8 below. The spectrum gap between 3500-1844 cm^{-1} presents the functional groups zone. The next part is the 500-1375 cm^{-1} gap called fingerprint zone. This last zone is responsible of composition changes of molecules into ZnS thin films. It is used usually in vibration analyses frequency. After the process of analyzing the FTIR spectra of ZnS samples, we noticed that there is no significant difference of effect of number of cycles on their functional groups. If we take the spectral band in wavenumber 792 cm^{-1}, we will find that is related to characteristic Zn-S stretching

which reflects its presence in ZnS thin films, which also comply with the work elaborated by T.Hurma et al [25]. The table below presents the peaks number of FTIR spectra of ZnS with assignments.

Table 2. *The peaks number of FTIR spectra of ZnS with assignments* [26].

Peaks number	Wavenumbers cm^{-1}	Assignments
1	1641	C=O stretching
2	1628	O-H bending
3	1452	C-C stretching
4	792	Zn-S stretching
5	737	C=S stretching
6	617	Cubic phase of ZnS

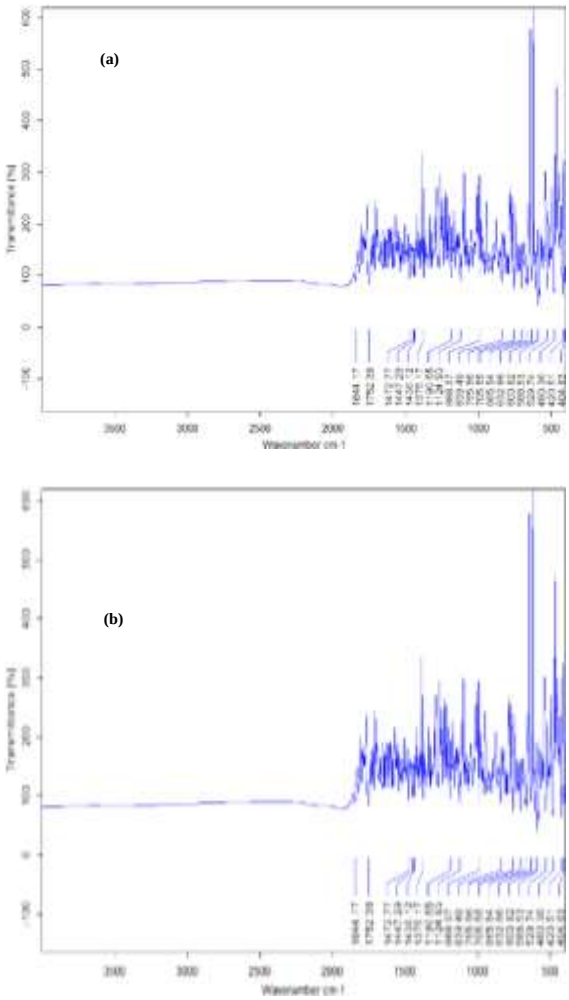

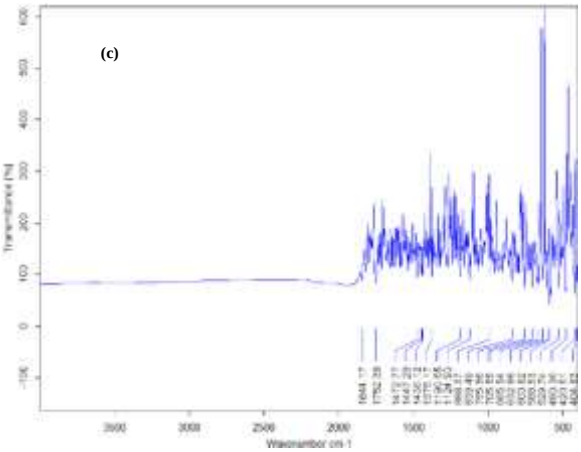

Figure 8*. FTIR spectra of ZnS samples: (a) 30 cycles, (b) 40 cycles and (c) 50 cycles deposited at room temperature.*

3.5. Electrical Characterization

In electrical characterization and in the hope to study the type of the conductivity of semiconductors: n-type or p-type, we use a simple technique named hot point prob. We use a voltameter and a heat source is placed in one of the leads of every ZnS sample. When we place the heat source on the positive lead of voltmeter, we noticed a positive voltage readied on the area of the voltameter, which will explain the n-type of our samples, and confirmed the literature of ZnS thin films [27, 28].

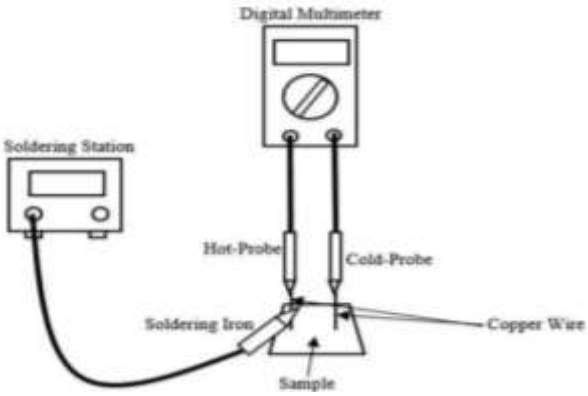

Figure *9. Conventional hot-point probe setup* [27].

Using Ohm meter, we can define the values of ZnS samples resistance then we conclude the values of resistivity. The

table below describes the effect of number of cycles on ZnS resistivity. We can notice that the resistivity of ZnS particles decreases from $0.661 \cdot 10^6$ to $0.4478 \cdot 10^6$ (Ω·cm) as layer thickness increases from 890 to 1780 nm, which is due to the decreasing in band gap energy of ZnS particles and in agreement with literature of the ZnS materials [28].

***Table 3**. Electrical resistivity and thickness film of ZnS samples.*

Number of cycles	Thickness (nm)	Resistivity ($\mathbf{x10^6\ \Omega.cm}$)
30	890	0.6610
40	1112	0.5335
50	1780	0.4478

When we made the growth process of ZnS thin film, we notice that increasing number of cycles affects an increasing of ZnS layer thickness, which means decreasing the resistivity of the film. In SEM micrographs, when we analyzed the composition molecules of ZnS semiconductors, we found some impurities appeared such as Oxygen (O) and Silicon (Si) with significant amount. The Zinc included in ZnS layers is probably impure because of existence of Oxygen with considerable quantity. As a reason, the resistivity values decreases when the Oxygen quantity increases.

4. CONCLUSION

In this paper, ZnS nanoparticles were deposited on glass substrate at room temperature. The morphology of the thin films showed relatively thick layers for 50 cycles. The XRD pattern reveals that the ZnS thin films were polycrystalline, having a cubic phase structure (Blende) with an orientation to (111) plane. Additionally, the grain size and the intensity of the diffraction peak increased with an increase in the number of cycles. The band gap energy for the deposited ZnS-SILAR thin film was in the range of 3.68–3.34 eV, which confirms its application as a buffer layer in solar cell second generation. The new result obtained in this study proves the finding of similar results in XRD, UV VIS Spectrophotometer and SEM EDX, with a minimal number of cycles contrary to other studies which necessitate passing up to 100 and 200 cycles to get the same intensity of diffraction peaks. By controlling this parameter, the structural and optical properties of ZnS thin films can be tailored for various devices.

ACKNOWLEDGEMENTS

We would like to thank Professors Mounir Fahoume and Khalid Nouneh for their collaboration in this work, especially in the Results and Discussions phase.

We would like to thank the Laboratory of Physics of Materials and Subatomic Physics, where we conducted the experiment on the effect of the number of cycles on a ZnS thin film using the SILAR technique.

REFERENCES

1. Santhamoorthy, A., Srinivasan, P., Krishnakumar, A., Rayappan, J., Babu, K. J., "SILAR-deposited nanostructured ZnO thin films: effect of deposition cycles on surface properties", *Bull. Mater. Sci.*, 44 (2021) 3.
2. Shobana, T. S. T., Venkatesan, T. V. T., Kathirvel, D. K. D., "A Comprehensive Review on Zinc Sulphide Thin Film by Chemical Bath Deposition Techniques", *J. Environ. Nanotechnol.*, 9 (2020) 50-59.
3. Naghavi, N., Abou-Ras, D., Allsop, N., Barreau, N., Bu¨ cheler, S., Ennaoui, A., Fischer, C.-H., Guillen, C., Hariskos, D., Herrero, J., Klenk, R., Kushiya, K., Lincot, D., Menner, R., Nakada, T., Platzer-Bjorkman, C., Spiering, S., Tiwari, A. N., rndahl, T. T., "Buffer layers and transparent conducting oxides for chalcopyrite $Cu(In,Ga)(S,Se)_2$ based thin film photovoltaics: Present status and current developments", *Prog. Photovoltaics Res. Appl.*, 18 (2010) 411-433.
4. Rahman, F., Podder, J., Ichimura, M., "Studies on Structural and Optical Characterization of In-Zn-S Ternary Thin Films Prepared by Spray Pyrolysis", *Int. J. Opt. Photonics*, 5 (2011) 79-86.
5. Yildiz, A., Yurduguzel, B., Kayhan, B., Calin, G., Dobromir, M., Iacomi, F., "Electrical conduction

properties of Co-doped ZnO nanocrystalline thin films", *J. Mater. Sci. Mater. Electron.*, 23 (2012) 425-430.
6. Borah, J. P., Sarma, K. C., "Optical and optoelectronic properties of ZnS nanostructured thin film", *Acta Phys. Pol. A.*, 114 (2008) 713-719.
7. Megersa Jigi, G., Abza, T., Girma, A., "Synthesis and characterization of aluminum dope zinc sulfide (Al:ZnS) thin films by chemical bath deposition techniques", *J. Appl. Biotechnol. Bioeng.*, 8 (2021) 55-58.
8. El Farri, H., Bouachri, M., Fahoume, M., Frimane, A., Daoudi, O. "Theoretical simulation of ZnS buffer layer thin films with SCAPS-1D software for photovoltaic applications", *Chalcogenide Lett.*, 18 (2021) 457-465.
9. Paire, M., Delbos, S., Vidal, J., Naghavi, N., Guillemoles, J. F., "*Chalcogenide Thin-Film Solar Cells*", (2014).
10. Patidar, D., Rathore, K. S., Saxena, N. S., Sharma, K., Sharma, T. P., "Energy band gap studies of cds nanomaterials", *J. Nano Res.*, 3 (2008) 97-102.
11. Elfarri, H., Bouachri, M., Frimane, A., Fahoume, M., Daoudi, O., Battas, M., "Optimization of simulations of thickness layers, temperature and defect density of CIS based solar cells, with SCAPS-1D software, for photovoltaic application", *Chalcogenide Lett.*, 18 (2021) 201-213.
12. Nisreen S. Turki, I. H., "Optical properties of ZnS and PEDOT thin films", *AIP Conf. Proceedings.*, (2021).
13. Bouachri, M., El Farri, H., Beraich, M., Taibi, M., Nouneh, K., Fahoume, M., "Influence of cycle numbers on optical parameters of nanostructured Bi2S3 thin films using SILAR method for solar cells light harvesting", *Materialia*, 20 (2021) 101-142.
14. AL-Tememee, N. A. A., Jawad, F. K., Jabor, A. A., "Effect of the Number of Dipping Cycles for a Cadmium Oxide Film Prepared by SILAR Method", *Ibn AL- Haitham J. Pure Appl. Sci.*, 35 (2022) 28-36.
15. Cheng, Y.-L., "Thin Films Processed by SILAR Method", *Intech*, 11 (2016) 13.
16. V. K. Ashith and K. Gowrish Rao, "Structural and Optical Properties of ZnS Thin Films by SILAR Technique obtained by acetate Precursor", *IOP Conf. Ser. Mater. Sci. Eng.*, 360 (2018) 1.
17. Lethobane, Manthako Hycinth., *"The synthesis and characterization of ZnS nanoparticles from zinc-based thiourea derivative complexes for potential use in photocatalysis"*. *Diss.*, (2017).
18. Odunaike, K., Adenijf, O. A., Sheu, A. L., Fowodu, T. O., Alabi, T. A., "Effect of different silar cycle on chemically deposited zinc copper sulphide (Zncus)", *Int. J. Thin Film Sci. Technol.*, (2021) 117-120.
19. Asghar, M., Mahmood, K., Samaa BM, Rabia, S., Shahid, M. Y., "Effect of Annealing Temperature on the Structural and Optical Properties of ZnS Thin Films", *Mater. Today Proc.*, 2 (2015) 5430-5435.
20. Bioki, H. A., Zarandi, M. B., "ZnS nanoparticles effect on electrical properties of Au/PANI-ZnS/Al heterojunction", *Int. J. Nanosci. Nanotechnol.*, 15 (2019) 45-53.
21. Dejan Zagorac, J. Z., "Band Gap Engineering of Newly Discovered ZnO/ZnS Polytypic Nanomaterials", *nanomaterials*, (2022) 1-20.
22. Ojha, K. S., "Structural and optical properties of PVA doped zinc sulphide thin films", *Optik (Stuttg).*, 127 (2016) 2586-2589.
23. Becker, F. G., "Covariance structural analysis of health-related indices in the elderly at home with a focus on subjective feelings of health", 7 (2015) 1.
24. Mohamed, S. H., Hadia, N. M. A., Awad, M. A., Shaaban, E. R., "Effects of thickness and Ag layer addition on the properties of ZnS thin films", *Acta Phys. Pol. A*, 135 (2019) 420-425.
25. Hurma, T., "The structural and optical properties of ZnS films optained by spraying solutions at different molarities", *Mater. Today Proc.*, 18 (2019) 1875-1881.
26. Selvakumar, C., Deepa, M., "Synthesis and characterization of silver-cadmium sulphide nanoparticles using wet chemical route", *Int. J. ChemTech Res.*, 7 (2014) 2675-2680.
27. Au, B. W. C., Chan, K. Y., Sin, Y. K., Ng, Z. N., "Hot-point probe measurements of N-type and P-type ZnO films", *Microelectron. Int.*, 34 (2017) 30-34.
28. Borse J., Garde, A., "Influence of complexing agent, pH of solution and thickness on morphological and optical properties of ZnS particles layer prepared by electrochemical deposition technique", *Nanosyst. Physics, Chem. Math.*, 11 (2020) 519-528.